HELICALLY DISTORTED RELATIVISTIC ELECTRON BEAM EQUILIBRIA FOR FREE ELECTRON LASER APPLICATIONS

Ronald C. Davidson

and

Han S. Uhm

July, 1980

PFC/JA-80-18

HELICALLY DISTORTED RELATIVISTIC ELECTRON BEAM EQUILIBRIA FOR FREE ELECTRON LASER APPLICATIONS

Ronald C. Davidson
Plasma Fusion Center
Massachusetts Institute of Technology
Cambridge, Massachusetts 02139

and

Science Applications Inc.
Boulder, Colorado 80302

Han S. Uhm
Naval Surface Weapons Center
White Oak, Silver Spring, Maryland 20910

ABSTRACT

The purpose of this paper is to develop a self-consistent kinetic description of helically distorted relativistic electron beam equilibria for free electron laser applications. In particular, radially confined equilibria are considered for a helically distorted electron beam propagating in the combined transverse wiggler and uniform axial guide fields described by $\underset{\sim}{B}^0=B_0\hat{\underset{\sim}{e}}_z+\delta\underset{\sim}{B}=B_0\hat{\underset{\sim}{e}}_z-\delta B\cos k_0 z\hat{\underset{\sim}{e}}_x-\delta B\sin k_0 z\hat{\underset{\sim}{e}}_y$, where $B_0=$ const., $\delta B=$const., and $\lambda_0=2\pi/k_0=$const. is the axial wavelength of the wiggler field. It is assumed that the beam density and current are sufficiently small that the equilibrium self fields can be neglected in comparison with $\underset{\sim}{B}^0$. In this context, it is found that there are three useful (and exact) invariants $(C_\perp,C_h,C_z)$ associated with single-particle motion in the equilibrium field $B_0\hat{\underset{\sim}{e}}_z+\delta\underset{\sim}{B}$. These invariants are used to construct radially confined Vlasov equilibria $f_b^0(C_\perp,C_h,C_z)$ for an intense relativistic electron beam propagating primarily in the z-direction. Examples of both solid and hollow beam equilibria are considered, and it is shown that the transverse wiggler field can have a large modulational influence on the beam envelope, depending on the size of $\delta B/B_0$.

I. INTRODUCTION

There have been several theoretical[1-5] and experimental[6,7] investigations of the free electron laser which generates coherent electromagnetic radiation using an intense relativistic electron beam as an energy source. With few exceptions, theoretical studies of the free electron laser instability are based on highly simplified models which neglect the influence of finite radial geometry and beam kinetic effects, or make use of very idealized approximations in analyzing the matrix dispersion equation. The purpose of this paper is to develop a self-consistent kinetic description of helically distorted relativistic electron beam equilibria for free electron laser applications. In particular, we consider radially confined Vlasov equilibria for a helically distorted relativistic electron beam propagating in the combined transverse wiggler and uniform axial guide fields described by [Eqs. (1) and (2)]

$$\underset{\sim}{B}^0 = B_0\hat{\underset{\sim}{e}}_z + \delta\underset{\sim}{B}$$

$$= B_0\hat{\underset{\sim}{e}}_z - \delta B\cos k_0 z\hat{\underset{\sim}{e}}_x - \delta B\sin k_0 z\hat{\underset{\sim}{e}}_y \ ,$$

where B_0=const., δB=const., and $\lambda_0 = 2\pi/k_0$=const. is the axial wavelength of the helical wiggler field. Both solid and hollow beam equilibria are considered, and it is assumed that the beam density and current are sufficiently small that equilibrium self fields can be neglected in comparison with $\underset{\sim}{B}^0$. Within the context of this assumption it is found that there are three useful (and exact) invariants $(C_\perp, C_h, C_z)$ associated with single-particle motion in the equilibrium field $B_0\hat{\underset{\sim}{e}}_z + \delta\underset{\sim}{B}$. These invariants can be used to construct radially confined Vlasov equilibria $f_b^0(C_\perp, C_h, C_z)$ for an intense relativistic electron beam

propagating in the z-direction, including the important modulational influence of the transverse wiggler field on the beam envelope.

The three exact invariants derived in Sec. II and Appendix A are given by the perpendicular invariant $C_\perp$ [Eq. (4)],

$$C_\perp = p_r^2 + p_\theta^2 + \frac{2eB_0}{ck_0}(p_z - \gamma_b m V_b) + \frac{2e}{ck_0}\underset{\sim}{p}_\perp \cdot \delta\underset{\sim}{B} \ ,$$

the helical invariant C_h [Eq. (5)],

$$C_h = P_\theta + \frac{1}{k_0}(p_z - \gamma_b m V_b) + \frac{er}{ck_0}\delta B \sin(\theta - k_0 z) \ ,$$

and the axial invariant C_z defined by [Eq. (6)]

$$\left(C_z - \frac{eB_0}{ck_0}\right)^2 = \left(p_z - \frac{eB_0}{ck_0}\right)^2 - \frac{2e}{ck_0}\underset{\sim}{p}_\perp \cdot \delta\underset{\sim}{B} \ ,$$

where $\underset{\sim}{p} = (p_r, p_\theta, p_z) = \gamma m \underset{\sim}{v}$ is the mechanical momentum, $P_\theta = r(p_\theta - eB_0 r/2c)$ is the canonical angular momentum, $\gamma_b mc^2 = \text{const.}$ is the characteristic directed energy of the electron beam, and $V_b = \text{const.}$ is the characteristic mean axial velocity. In the expressions for $C_\perp$ and C_h, we have subtracted the constant terms proportional to $\gamma_b m V_b$ without loss of generality. Moreover, for $\delta\underset{\sim}{B} = 0$, we note from Eq. (6) that the axial momentum p_z is a constant of the motion, and that Eqs. (4) and (5) yield the familiar invariants, $p_r^2 + p_\theta^2 = \text{const.}$ and $P_\theta = \text{const.}$, for a charged particle moving in a uniform axial field B_0.

The striking feature of the present analysis is the fact that the exact invariants $(C_\perp, C_h, C_z)$ can be used to construct helically distorted relativistic electron beam equilibria $f_b^0(C_\perp, C_h, C_z)$ of experimental interest for free electron laser applications. Generally speaking, the two classes of relevant beam equilibria can be characterized as (a) solid beam equilibria, and (b) hollow beam equilibria. For example, equilibrium distribution functions of the form [Eq. (10)]

$$f_b^0=F_1(C_\perp-2\gamma_b m\omega_b C_h)G(C_z) \ ,$$

where $G(C_z)$ is strongly peaked around $C_z=\gamma_b mV_b$, correspond to a solid electron beam with non-zero density on axis (r=0). On the other hand, the class of beam equilibria described by [Eq. (11)]

$$f_b^0=F_2(C_\perp)\delta(C_h-C_0)G(C_z) \ ,$$

where $C_0=-(eB_0/2c)R_0^2=$const., corresponds to a slowly rotating annular electron beam with characteristic mean radius R_0. Of course, it is found that the detailed spatial dependence of beam equilibrium properties (density profile, temperature profile, etc.) depends on the specific functional form of $G(C_z)$, $F_2(C_\perp)$ and $F_1(C_\perp-2\gamma_b m\omega_b C_h)$. It is also found that the radial envelope of the beam can be strongly modulated by the transverse wiggler field, depending on the size of $\delta B/B_0$ [Sec. III].

As a general remark, one of the most appealing features of the recent free electron laser stability analyses by Davidson and Uhm,[3] Sprangle and Smith,[5] and Bernstein and Hirshfield[4] for a relativistic electron beam with uniform density and infinite cross-section is the fact that the influence of the transverse wiggler field is contained in a fully self-consistent manner in the equilibrium distribution function $f_b^0=n_0\delta(P_x)\delta(P_y)G_0(p_z)$. That is, when carrying out the stability analysis, the excited electromagnetic and electrostatic fields are treated as small-amplitude perturbations about a self-consistent equilibrium that includes the full nonlinear influence of the equilibrium wiggler field. We believe that the present equilibrium investigations form an important first step in formulating a self-consistent Vlasov description of the free electron laser instability that includes the effects of finite radial geometry and also correctly incorporates

the nonlinear influence of the transverse wiggler field on the beam equilibrium.

The organization of this paper is the following. In Sec. II, we discuss the basic equilibrium configuration and assumptions. Specific examples of helically modulated relativistic electron beam equilibria are analyzed in Sec. III, both for solid [Sec. III.A] and hollow [Sec. III.B] electron beams.

II. EQUILIBRIUM CONFIGURATION AND BASIC ASSUMPTIONS

We consider the class of helically modulated relativistic electron beam equilibria propagating in an externally applied magnetic field

$$\underset{\sim}{B}^0 = B_0 \hat{\underset{\sim}{e}}_z + \delta\underset{\sim}{B} \ , \tag{1}$$

where B_0=const. is the axial magnetic field, and

$$\delta\underset{\sim}{B} = -\delta B \cos k_0 z \hat{\underset{\sim}{e}}_x - \delta B \sin k_0 z \hat{\underset{\sim}{e}}_y \ , \tag{2}$$

is the transverse helical wiggler field with axial wavelength $\lambda_0 = 2\pi/k_0$. In the present analysis, we assume that δB=const. is a good approximation over the radial extent of the beam. In cylindrical polar coordinates (r,θ,z), Eq. (2) can also be expressed as

$$\begin{aligned} \delta\underset{\sim}{B} &= \delta B_r \hat{\underset{\sim}{e}}_r + \delta B_\theta \hat{\underset{\sim}{e}}_\theta \\ &= -\delta B \cos(\theta - k_0 z)\hat{\underset{\sim}{e}}_r + \delta B \sin(\theta - k_0 z)\hat{\underset{\sim}{e}}_\theta \ , \end{aligned} \tag{3}$$

where $\hat{\underset{\sim}{e}}_r$ and $\hat{\underset{\sim}{e}}_\theta$ are unit vectors in the r- and θ-directions, respectively. It is assumed that the beam density and current are sufficiently low that the influence of the equilibrium self electric and self magnetic fields, $\underset{\sim}{E}_s^0(\underset{\sim}{x})$ and $\underset{\sim}{B}_s^0(\underset{\sim}{x})$, on the particle trajectories can be neglected in comparison with the $\underset{\sim}{v}\times\underset{\sim}{B}^0$ force associated with the applied magnetic field in Eq. (1).

Within the context of the above assumptions, there are three useful and exact invariants $(C_\perp, C_h, C_z)$ associated with single-particle motion in the equilibrium field $B_0\hat{\underset{\sim}{e}}_z + \delta\underset{\sim}{B}$. These invariants can be used to construct cylindrical Vlasov equilibria $f_b^0(C_\perp, C_h, C_z)$ for an intense relativistic electron beam propagating in the z-direction, including the important modulational influence of the transverse wiggler field

on the beam envelope. As outlined in Appendix A, for relativistic electron motion in the applied magnetic field defined in Eqs. (1) and (2), the three exact invariants are given by the transverse invariant $C_\perp$ [Eq. (A.12)],

$$C_\perp = p_r^2 + p_\theta^2 + \frac{2eB_0}{ck_0}(p_z - \gamma_b m V_b) + \frac{2e}{ck_0} \underset{\sim}{p}_\perp \cdot \delta \underset{\sim}{B} , \tag{4}$$

the helical invariant C_h [Eq. (A.7)],

$$C_h = P_\theta + \frac{1}{k_0}(p_z - \gamma_b m V_b) + \frac{e\delta B}{ck_0} r\sin(\theta - k_0 z) , \tag{5}$$

and the axial invariant C_z defined by [Eq. (A.11)],

$$\left(C_z - \frac{eB_0}{ck_0}\right) = \left(p_z - \frac{eB_0}{ck_0}\right)^2 - \frac{2e}{ck_0} \underset{\sim}{p}_\perp \cdot \delta \underset{\sim}{B} . \tag{6}$$

In Eqs. (4)-(6), $\underset{\sim}{p} = (p_r, p_\theta, p_z) = \gamma m \underset{\sim}{v}$ is the mechanical momentum, $P_\theta = r(p_\theta - eB_0 r/2c)$ is the canonical angular momentum associated with the axial field B_0, $\gamma mc^2 = (m^2c^4 + c^2 \underset{\sim}{p}^2)^{1/2}$ is the relativistic electron energy, $-e$ is the electron charge, m is the electron rest mass, $\gamma_b mc^2 = $ const. is the characteristic directed energy of the electron beam, and $V_b = $ const. is the characteristic mean axial velocity. Moreover, $\underset{\sim}{p}_\perp$ is the transverse momentum, and $\underset{\sim}{p}_\perp \cdot \delta \underset{\sim}{B}$ can be expressed as $\underset{\sim}{p}_\perp \cdot \delta \underset{\sim}{B} = -p_r \delta B \cos(\theta - k_0 z) + p_\theta \delta B \sin(\theta - k_0 z)$. Note in Eqs. (4) and (5) that we have subtracted the constant terms proportional to $\gamma_b m V_b$ without loss of generality. For $B_0 = $ const. and $\delta B = $ const., we reiterate that $C_\perp$, C_h, and C_z are <u>exact</u> constants of the motion for arbitrary wiggler amplitude δB.

In the limit of zero wiggler amplitude, $\delta B \to 0$, Eqs. (4)-(6) reduce to

$$C_\perp^0 = p_r^2 + p_\theta^2 + \frac{2eB_0}{ck_0}(p_z - \gamma_b m V_b) = \text{const.}, \tag{7}$$

$$C_h^0=P_\theta+\frac{1}{k_0}(p_z-\gamma_b mV_b)=\text{const.}, \tag{8}$$

$$C_z^0=p_z=\text{const.} \tag{9}$$

For $\delta B=0$, we note from Eq. (9) that the axial momentum p_z is a constant of the motion, and Eqs. (7) and (8) yield the familiar invariants, $p_r^2+p_\theta^2=\text{const.}$ and $P_\theta=\text{const.}$, for a charged particle moving in a uniform axial field B_0.

There are two classes of helical beam equilibria $f_b^0(C_\perp,C_h,C_z)$ of experimental interest for free electron laser applications. Generally speaking, the two classes can be characterized as (a) solid beam equilibria, and (b) hollow beam equilibria. For example, equilibrium distribution functions of the form

$$f_b^0=F_1(C_\perp-2\gamma_b m\omega_b C_h)G(C_z)\ , \tag{10}$$

where $G(C_z)$ is strongly peaked around $C_z=\gamma_b mV_b$, corresponds to a solid electron beam with non-zero density on axis (r=0). In Eq. (10), $\omega_b=\text{const.}$ is related to the mean angular rotation of the beam [Sec. III]. On the other hand, the class of beam equilibria described by

$$f_b^0=F_2(C_\perp)\delta(C_h-C_0)G(C_z)\ , \tag{11}$$

where $C_0=-(eB_0/2c)R_0^2=\text{const.}$, corresponds to a slowly rotating annular electron beam with characteristic mean radius R_0. Of course, the detailed spatial dependence of the beam equilibrium properties (e.g., density profile, temperature profile, etc.) depends on the specific functional form of $G(C_z)$, $F_1(C_\perp-2\gamma_b m\omega_b C_h)$ and $F_2(C_\perp)$. In this regard, specific examples of helical beam equilibria are discussed in Sec. III. As a general remark, it is found that the radial extent of the beam can be strongly modulated by the transverse wiggler field, depending

on the size of $\delta B/B_0$.

While it is true that beam equilibrium properties can be calculated from Eqs. (10) and (11) making use of the exact invariants in Eqs. (4)-(6), there are useful approximations that can be made in simplifying the expression for C_z [Eq. (6)] in the regimes of practical interest for free electron laser applications. We now discuss these approximations, which will be used in the detailed equilibrium examples presented in Sec. III.

First, in the regimes of practical interest, the characteristic transverse momentum $\underset{\sim}{p}_\perp$ of a beam electron is small in comparison with the characteristic directed axial momentum $\gamma_b mV_b \hat{z} \simeq p_z$, i.e.,

$$|\underset{\sim}{p}_\perp| << \gamma_b mV_b \ . \tag{12}$$

Second, we assume that the beam axial motion is far removed from cyclotron resonance. Specifically, referring to Eq. (6), it is assumed that

$$\left|\gamma_b mV_b - \frac{eB_0}{ck_0}\right|^2 >> \frac{2e}{ck_0} \ |\underset{\sim}{p}_\perp \cdot \delta\underset{\sim}{B}|, \tag{13}$$

or equivalently,

$$|\omega_0 - \omega_c|^2 >> 2\omega_c\omega_0 \left|\frac{\underset{\sim}{p}_\perp}{\gamma_b mV_b} \cdot \frac{\delta\underset{\sim}{B}}{B_0}\right| \ , \tag{14}$$

where ω_0 and ω_c are defined by

$$\omega_0 = k_0 V_b \text{ and } \omega_c = \frac{eB_0}{\gamma_b mc} \ . \tag{15}$$

To assure radial confinement of the beam electrons, the present analysis of course assumes $B_0 \neq 0$. Making use of the inequality $|\underset{\sim}{p}_\perp| << \gamma_b mV_b$ [Eq. (12)], the striking feature of the present analysis is that the inequality in Eq. (14) is easily satisfied even for large wiggler amplitude ($\delta B \gtrsim B_0$, say), both in the limits of weak axial field

($\omega_c^2 \ll \omega_0^2$) and strong axial field ($\omega_c^2 \gg \omega_0^2$). For example, if $\omega_0^2 \gg \omega_c^2$, then Eq. (14) reduces to

$$1 \gg 2 \frac{\omega_c}{\omega_0} \left| \frac{\underset{\sim}{p}_\perp}{\gamma_b m V_b} \cdot \frac{\delta \underset{\sim}{B}}{B_0} \right| \quad , \tag{16}$$

which is readily satisfied in the parameter regimes of experimental interest. In any case, within the context of the inequalities in Eqs. (12) and (13), the exact axial invariant C_z defined in Eq. (6) can be approximated by

$$C_z = p_z - \frac{\frac{e}{ck_0} \underset{\sim}{p}_\perp \cdot \delta \underset{\sim}{B}}{p_z - \frac{eB_0}{ck_0}} \quad , \tag{17}$$

where we have taken the positive square root in Eq. (6), which corresponds to C_z and p_z having the same polarity. Equation (17) is an excellent approximation to C_z in the parameter regimes of practical interest for free electron laser applications. Moreover, for $G(C_z)$ strongly peaked about $C_z = \gamma_b m V_b$, with characteristic half-width $\Delta C_z \ll \gamma_b m V_b$, the denominator on the right-hand side of Eq. (17) can be approximated by $p_z - eB_0/ck_0 = \gamma_b m V_b - eB_0/ck_0$. Equation (17) then reduces to

$$C_z = p_z - \frac{\omega_c}{\omega_0 - \omega_c} \underset{\sim}{p}_\perp \cdot \frac{\delta \underset{\sim}{B}}{B_0} \quad , \tag{18}$$

which is the approximate form of the axial invariant used in Sec. III.

III. EXAMPLES OF HELICALLY MODULATED RELATIVISTIC ELECTRON BEAM EQUILIBRIA

There is clearly a wide variety of helically modulated relativistic electron beam equilibria that can be analyzed within the context of the equilibrium formalism described in Sec. II. The relevant choice of $f_b^0(C_\perp, C_h, C_z)$ of course depends in detail on injection geometry, beam quality, etc. For our purposes here, we consider two simple examples of solid and hollow beam equilibria that clearly illustrate the strong influence of the transverse wiggler field in modulating the beam envelope. In both cases, for simplicity, we assume that the axial distribution $G(C_z)$ is cold, i.e.,

$$\begin{aligned} G(C_z) &= \delta(C_z - \gamma_b m V_b) \\ &= \delta\left(p_z - \gamma_b m V_b - \frac{\omega_c}{\omega_0 - \omega_c}\, \underset{\sim}{p}_\perp \cdot \frac{\delta \underset{\sim}{B}}{B_0}\right) , \end{aligned} \tag{19}$$

where use has been made of Eq. (18). The analysis can be extended in a straightforward manner to distribution functions $G(C_z)$ with a small spread about $C_z = \gamma_b m V_b$.

A. Solid Beam Equilibria

As an example of a helically modulated solid electron beam, we consider the case where $f_b^0(C_\perp, C_h, C_z)$ has the form [Eq. (10)]

$$\begin{aligned} f_b^0 = \frac{n_0}{\pi}\, &\delta(C_\perp - 2\gamma_b m \omega_b C_h - 2\gamma_b m \hat{T}_\perp) \\ &\times \delta(C_z - \gamma_b m V_b) , \end{aligned} \tag{20}$$

where $C_\perp$ and C_h are defined in Eqs. (4) and (5), C_z is defined in Eq. (18), and n_0, ω_b, and $\hat{T}_\perp$ are positive constants. Equation (20)

is a straightforward generalization of the uniform density beam equilibrium $f_b^0=(n_0/\pi)\delta(p_r^2+p_\theta^2-2\gamma_b m\omega_b P_\theta-2\gamma_b m\hat{T}_\perp)\delta(p_z-\gamma_b mV_b)$ previously discussed by Davidson[8] for the case $\delta B=0$. Evaluating $C_\perp-2\gamma_b m\omega_b C_h$ for $C_z=\gamma_b mV_b$, and rearranging terms, we find that

$$[C_\perp-2\gamma_b m\omega_b C_h]_{C_z=\gamma_b mV_b}$$

$$=\left(p_r+\frac{e}{ck_0}\left(\frac{\omega_0-\omega_b}{\omega_0-\omega_c}\right)\delta B_r\right)^2+\left(p_\theta-\gamma_b m\omega_b r+\frac{e}{ck_0}\left(\frac{\omega_0-\omega_b}{\omega_0-\omega_c}\right)\delta B_\theta\right)^2$$

$$+\gamma_b^2 m^2\psi(r,\theta-k_0z)\ , \tag{21}$$

where $\omega_0=k_0V_b$, $\omega_c=eB_0/\gamma_b mc$, $\delta B_r=-\delta B\cos(\theta-k_0z)$, $\delta B_\theta=\delta B\sin(\theta-k_0z)$, and the effective potential $\psi(r,\theta-k_0z)$ is defined by

$$\psi(r,\theta-k_0z)=(\omega_b\omega_c-\omega_b^2)r^2$$

$$+2\omega_c\omega_b\left(\frac{\omega_c-\omega_b}{\omega_0-\omega_c}\right)\frac{r}{k_0}\frac{\delta B}{B_0}\sin(\theta-k_0z)-\left(\frac{\omega_0-\omega_b}{\omega_0-\omega_c}\right)^2\frac{\omega_c^2}{\omega_0^2}\left(\frac{\delta B}{B_0}\right)^2V_b^2\ . \tag{22}$$

We now evaluate various macroscopic properties of physical interest for the choice of distribution function in Eq. (20). For example, making use of Eqs. (20) and (21), it is readily shown that the equilibrium density profile $n_b^0(r,\theta,z)=\int d^3p\ f_b^0(C_\perp,C_h,C_z)$ corresponds to a constant-density beam with sharp radial boundaries, i.e.,

$$n_b^0(r,\theta-k_0z)=\begin{cases} n_0\ , & \psi(r,\theta-k_0z)\leq 2\hat{T}_\perp/\gamma_b m\ , \\ 0\ , & \psi(r,\theta-k_0z)>2\hat{T}_\perp/\gamma_b m\ , \end{cases} \tag{23}$$

where ψ is defined in Eq. (22). Moreover, making use of $|p_\perp|<\gamma_b mV_b$, the mean equilibrium velocity of the electron beam can be approximated by

$$V_b^0(\underset{\sim}{x})=[\int d^3p(\underset{\sim}{p}/\gamma m)f_b^0]/(\int d^3p\ f_b^0)$$

$$\simeq \frac{1}{\gamma_b m}\ (\int d^3p\ \underset{\sim}{p}\ f_b^0)/(\int d^3p\ f_b^0)\ , \tag{24}$$

and the transverse temperature profile can be approximated by

$$T_{\perp b}^0(\underset{\sim}{x})=\frac{1}{2}\ \{\int d^3p[(p_r-\langle p_r\rangle)(v_r-\langle v_r\rangle)+(p_\theta-\langle p_\theta\rangle)(v_\theta-\langle v_\theta\rangle]f_b^0\}/(\int d^3p f_b^0)$$

$$\simeq \frac{1}{2\gamma_b m}\ \{\int d^3p[(p_r-\langle p_r\rangle)^2+(p_\theta-\langle p_\theta\rangle)^2]f_b^0\}/(\int d^3p f_b^0)\ , \tag{25}$$

where $\langle p_j\rangle=(\int d^3p p_j f_b^0)/(\int d^3p f_b^0)$, and use has been made of $\gamma\simeq\gamma_b$. Substituting Eqs. (20) and (21) into Eq. (24), the mean macroscopic velocity components of the electron beam can be expressed as

$$V_{rb}^0(r,\theta-k_0z)=V_b\ \frac{\omega_c}{\omega_0}\left(\frac{\omega_0-\omega_b}{\omega_0-\omega_c}\right)\frac{\delta B}{B_0}\cos(\theta-k_0z)\ , \tag{26}$$

$$V_{\theta b}^0(r,\theta-k_0z)=\omega_b r-V_b\ \frac{\omega_c}{\omega_0}\left(\frac{\omega_0-\omega_b}{\omega_0-\omega_c}\right)\frac{\delta B}{B_0}\sin(\theta-k_0z)\ , \tag{27}$$

and

$$V_{zb}^0(r,\theta-k_0z)=V_b\ , \tag{28}$$

in the region of configuration space where $n_b^0(r,\theta-k_0z)$ is non-zero. In obtaining Eqs. (26) and (27), use has been made of $\delta B_r=-\delta B\cos(\theta-k_0z)$ and $\delta B_\theta=\delta B\sin(\theta-k_0z)$, and the contribution to V_{zb}^0 of order $\langle\underset{\sim}{p}_\perp\rangle\cdot\delta\underset{\sim}{B}/\gamma_b m V_b B_0$ has been neglected in obtaining Eq. (28). Finally, making use of Eqs. (20), (21), and (25), the transverse temperature profile can be expressed as

$$T_{\perp b}^0(r,\theta-k_0z)=\hat{T}_\perp\left(1-\frac{\psi(r,\theta-k_0z)}{v_0^2}\right) \tag{29}$$

in the region of configuration space where $n_b^0(r,\theta-k_0z)$ is non-zero, i.e., where $\psi \le 2\hat{T}_\perp/\gamma_b m \equiv v_0^2$ [Eq. (23)].

Evidently, from Eq. (23), the outer radius $R_b(\theta-k_0z)$ of the electron beam is determined self-consistently from the solution to the "envelope" equation $\psi(R_b,\theta-k_0z)=2T_\perp/\gamma_b m \equiv v_0^2$. Making use of Eq. (22), we find that the physically allowed value of $R_b(\theta-k_0z)$ is given by the expression

$$R_b(\theta-k_0z)=\Delta R_b \sin(\theta-k_0z)+[(\Delta R_b)^2\sin^2(\theta-k_0z)+R_0^2]^{1/2} , \qquad (30)$$

where R_0 and ΔR_b are defined by

$$R_0^2= \frac{\left[v_0^2+\left(\frac{\omega_0-\omega_b}{\omega_0-\omega_c}\right)^2 \frac{\omega_c^2}{\omega_0^2}\left(\frac{\delta B}{B_0}\right)^2 v_b^2\right]}{(\omega_b\omega_c-\omega_b^2)} , \qquad (31)$$

and

$$k_0\Delta R_b= \frac{\omega_c}{\omega_0-\omega_c}\frac{\delta B}{B_0} . \qquad (32)$$

Moreover, the equilibrium density profile in Eq. (23) can be expressed as

$$n_b^0(r,\theta-k_0z)= \begin{cases} n_0 , & 0 < r \leq R_b(\theta-k_0z) , \\ 0 , & r > R_b(\theta-k_0z) . \end{cases} \qquad (33)$$

In addition, after some straightforward algebraic manipulation that makes use of Eqs. (29)-(32), the transverse temperature profile can be expressed as

$$T_{\perp b}^0(r,\theta-k_0z)=T_{\perp b}^m \frac{\left(1-\frac{r}{R_b}\right)\left(1+\frac{r}{R_b}-\frac{2\Delta R_b}{R_b}\sin(\theta-k_0z)\right)}{\left(1-\frac{2\Delta R_b}{R_b}\sin(\theta-k_0z)\right)} \qquad (34)$$

where $R_b(\theta-k_0z)$ is defined in Eq. (30), and $T_{\perp b}^m$ is the maximum, on-axis (r=0), transverse temperature defined by

$$T_{\perp b}^m=\hat{T}_\perp+\frac{\gamma_b m}{2}\left(\frac{\omega_0-\omega_b}{\omega_0-\omega_c}\right)^2 \frac{\omega_c^2}{\omega_0^2}\left(\frac{\delta B}{B_0}\right)^2 v_b^2 . \qquad (35)$$

As a simple reference equilibrium, for $\delta B=0$, we note from Eqs. (30) and (31) that the beam radius R_b reduces to the familiar

result[8] $R_b=R_0=v_0/(\omega_b\omega_c-\omega_b^2)^{1/2}$, and that $\Delta R_b=0$, which corresponds to zero modulation of the beam envelope. In addition, for $\delta B=0$, it follows that $V_{rb}^0=0$ [Eq. (26)], $V_{\theta b}^0=\omega_b r$ [Eq. (27)], and $T_{\perp b}^0=\hat{T}_\perp(1-r^2/R_0^2)$ [Eqs. (34) and (35)]. That is, for zero wiggler amplitude, Eqs. (30)-(35) reduce to the familiar results[8] corresponding to an electron beam with uniform density, constant beam radius, rigid-rotor angular velocity profile, and parabolic transverse temperature profile.

In the case where $\delta B\neq 0$, we note from Eqs. (30)-(32) that the outer envelope of the beam is modulated by the transverse wiggler field. Moreover, for existence of the equilibrium, $R_0^2 > 0$ is required [Eq. (31)] so that ω_b must lie in the range

$$0 < \omega_b < \omega_c \ , \tag{36}$$

for radially confined equilibria. From Eq. (30), the maximum (R_b^0) and minimum (R_b^i) radial excursion of the beam envelope occurs for $\theta-k_0z=(2n+1)\pi/2$, $n=0, \pm1, \pm2,\ldots$, with R_b^0 and R_b^i defined by

$$R_b^0=|\Delta R_b|+[(\Delta R_b)^2+R_0^2]^{1/2} \ ,$$

and (37)

$$R_b^i=-|\Delta R_b|+[(\Delta R_b)^2+R_0^2]^{1/2} \ ,$$

where R_0 and ΔR_b are defined in Eqs. (31) and (32), respectively. Defining the <u>average</u> beam radius by $\bar{R}_b=(R_b^0-R_b^i)/2$ gives

$$\bar{R}_b=[(\Delta R_b)^2+R_0^2]^{1/2} \ . \tag{38}$$

Moreover, defining the peak amplitude of the radial modulation by $\Delta\bar{R}_b=(R_b^0-R_b^i)/2$ gives

$$\overline{\Delta R}_b = |\Delta R_b|$$

$$= \left| \frac{1}{k_0} \frac{\omega_c}{\omega_0 - \omega_c} \frac{\delta B}{B_0} \right| . \tag{39}$$

We now parameterize the equilibrium properties within the context of the basic assumptions enumerated in Sec. II. First, the transverse (r,θ) motion is assumed to be nonrelativistic [Eq. (12)]. Making use of $|V^0_{rb}|$, $|V^0_{\theta b}| \ll c$, we find from Eqs. (26) and (27) that the quantities ω_c, ω_b, δB, etc. are required to satisfy

$$\left| \frac{V_b}{c} \frac{\omega_c}{\omega_0} \frac{(\omega_0 - \omega_b)}{(\omega_0 - \omega_c)} \frac{\delta B}{B_0} \right| \ll 1 , \tag{40}$$

and

$$\frac{\omega_b^2 \bar{R}_b^2}{c^2} \ll 1 , \tag{41}$$

where ω_0 and ω_c are far removed from cyclotron resonance [Eq. (14)]. For a weak axial field with $\omega_0 \gg \omega_c > \omega_b$, Eq. (40) reduces to

$$\left| \frac{V_b}{c} \frac{\omega_c}{\omega_0} \frac{\delta B}{B_0} \right| \ll 1 , \tag{42}$$

which is easily satisfied even for <u>moderate</u> wiggler amplitudes with $|\delta B/B_0| \gtrsim 1$. On the other hand, for a strong axial field with $\omega_0 \ll \omega_c$, Eq. (40) reduces to

$$\left| \frac{V_b}{c} \frac{\delta B}{B_0} \right| \ll 1, \tag{43}$$

which requires a <u>small</u> wiggler amplitude with $|\delta B/B_0| \ll 1$. Here we have assumed $\omega_0 > \omega_b$. Finally, for present purposes, we estimate $\omega_b^2 \bar{R}_b^2/c^2 \gtrsim \omega_b^2 R_0^2/c^2 \gtrsim \omega_b^2 v_0^2/\omega_b \omega_c c^2$ [Eq. (31)]. The inequality in Eq. (41) then becomes

$$\left| \frac{\omega_b}{\omega_c} \frac{v_0^2}{c^2} \right| \ll 1 , \tag{44}$$

which is easily satisfied since $\omega_b < \omega_c$ [Eq. (36)] and the transverse thermal motion is nonrelativistic ($v_0^2 << c^2$).

It is also interesting to determine the characteristic size of $k_0\bar{\Delta}R_b$, the normalized maximum radial excursion of the beam envelope. From Eq. (39), for $\omega_0 >> \omega_c$, we find $k_0\bar{\Delta}R_b \simeq |(\omega_c/\omega_0)(\delta B/B_0)| << 1$ [Eq. (42)] for weak axial magnetic field. Moreover, for $\omega_0 << \omega_c$, we find $k_0\bar{\Delta}R_b \simeq |\delta B/B_0| << 1$ [Eq. (43)] for strong axial magnetic field. That is,

$$k_0\bar{\Delta}R_b << 1 , \tag{45}$$

follows consistently from the assumption of nonrelativistic transverse motion in both the weak field [Eq. (42)] and strong field [Eq. (43)] regimes.

We also determine the characteristic size of k_0R_0. Estimating $R_0^2 \approx v_0^2/\omega_b\omega_c$ [Eq. (31)] gives

$$k_0^2R_0^2 = \frac{\omega_0^2}{\omega_b\omega_c}\frac{v_0^2}{V_b^2} , \tag{46}$$

where $\omega_0=k_0V_b$ and $\omega_b < \omega_c$ [Eq. (36)]. The regime of most interest experimentally is $k_0^2R_0^2 > 1$, which requires sufficiently slow beam rotation satisfying [Eq. (46)]

$$\frac{\omega_b}{\omega_c} < \frac{\omega_0^2}{\omega_c^2}\frac{v_0^2}{V_b^2} . \tag{47}$$

As a numerical example, in Fig. 1 we show a plot of the normalized radius k_0R_b of the beam envelope [Eq. (30)] versus $\theta-k_0z$ for several values of $\delta B/B_0$ and the choice of equilibrium parameters $\omega_0=4\omega_c$, $\omega_b=0.1\ \omega_c$, $v_0^2/c^2=0.04$, $\gamma_b=3$ and $V_b^2/c^2=8/9$. In this case,

$$k_0\Delta R_b = \frac{1}{3}\frac{\delta B}{B_0} , \tag{48}$$

and

$$k_0^2 R_0^2 = 8[1+\frac{1}{2}(19.5/9)^2(\delta B/B_0)^2] \tag{49}$$

follow from Eqs. (31) and (32). Substituting Eqs. (48) and (49) into the expression for R_b in Eq. (30) gives the results shown in Fig. 1 for $\delta B/B_0=1/4$ [Fig. 1(a)], $\delta B/B_0=0.5$ [Fig. 1(b)] and $\delta B/B_0=1$ [Fig. 1(c)]. We note from Eqs. (38), (39), (48), (49), and Fig. 1 that the normalized average beam radius $k_0\bar{R}_b$ and maximum modulation amplitude $k_0\bar{\Delta R}_b$ increase from $(k_0\bar{R}_b, k_0\bar{\Delta R}_b)=(2.83,0)$ for $\delta B/B_0=0$, to $(k_0\bar{R}_b, k_0\bar{\Delta R}_b)=$ (5.185, 0.333) for $\delta B/B_0=1$.

We conclude this section by emphasizing that the theoretical model developed here can be used to calculate the equilibrium properties of a helically modulated solid electron beam propagating in an equilibrium magnetic field prescribed by Eqs. (1) and (2) for a broad range of system parameters ω_b, ω_c, ω_0, v_0^2/c^2, $\delta B/B_0$, etc. The major approximations relate to the assumptions that the transverse particle motion is nonrelativistic [Eq. (12)] and that the axial motion is far removed from cyclotron resonance [Eq. (14)].

B. Annular Electron Beam

As an example of a helically modulated annular electron beam, we consider the case where $f_b^0(C_\perp, C_h, C_z)$ has the form [Eq. (11)]

$$f_b^0 = \frac{n_0 R_0 \gamma_b m v_0}{2\varepsilon} U[(C_\perp - \gamma_b^2 m^2 v_0^2)^2 - \varepsilon^2]\delta(C_h - C_0)\delta(C_z - \gamma_b m V_b) \ , \tag{50}$$

where $C_0 = -eB_0 R_0^2/2c = \text{const.}$, and n_0, R_0, v_0, and ε are positive constants. In Eq. (50), $U(x)$ is the Heaviside step function defined by $U(x)=1$ for $x > 0$, and $U(x)=0$ for $x < 0$. Evaluating $C_h - C_0$ and $C_\perp - (\gamma_b m v_0)^2$ at $C_z = \gamma_b m V_b$, and rearranging terms, we find

$$[C_h - C_0]_{C_z=\gamma_b m V_b} = \left(r + \frac{1}{k_0}\frac{\omega_c}{\omega_0 - \omega_c}\frac{\delta B}{B_0}\sin(\theta - k_0 z)\right) p_\theta' - \frac{1}{k_0}\frac{\omega_c}{\omega_0 - \omega_c}\frac{\delta B}{B_0}\cos(\theta - k_0 z) p_r' - F(r, \theta - k_0 z) \ , \tag{51}$$

and

$$[C_\perp - (\gamma_b m v_0)^2]_{C_z=\gamma_b m V_b} = p_r'^2 + p_\theta'^2 - (\gamma_b m)^2 v_0'^2 \ , \tag{52}$$

where

$$v_0'^2 = v_0^2 + V_b^2 \left(\frac{\omega_c}{\omega_0 - \omega_c}\right)^2 \left(\frac{\delta B}{B_0}\right)^2 \ ,$$

$$p_r' = p_r - \gamma_b m V_b \frac{\omega_c}{\omega_0 - \omega_c}\frac{\delta B}{B_0}\cos(\theta - k_0 z) \ , \tag{53}$$

$$p_\theta' = p_\theta + \gamma_b m V_b \frac{\omega_c}{\omega_0 - \omega_c}\frac{\delta B}{B_0}\sin(\theta - k_0 z) \ ,$$

and $F(r, \theta - k_0 z)$ is defined by

$$F = \gamma_b m V_b \left[\frac{1}{2}\frac{\omega_c}{\omega_0} k_0 (r^2 - R_0^2) + r\frac{\omega_c}{\omega_0}\frac{\omega_c}{\omega_0 - \omega_c}\frac{\delta B}{B_0}\sin(\theta - k_0 z) + \frac{1}{k_0}\left(\frac{\omega_c}{\omega_0 - \omega_c}\right)^2 \left(\frac{\delta B}{B_0}\right)^2\right] \ . \tag{54}$$

It is convenient to introduce the quantities f and g defined by

$$f=\frac{1}{k_0}\frac{\omega_c}{\omega_0-\omega_c}\frac{\delta B}{B_0}\sin(\theta-k_0z)\ ,$$
$$g=\frac{1}{k_0}\frac{\omega_c}{\omega_0-\omega_c}\frac{\delta B}{B_0}\cos(\theta-k_0z)\ . \tag{55}$$

Furthermore, evaluating $C_\perp-(\gamma_b mv_0)^2$ at $C_h=C_0$ and $C_z=\gamma_b mV_b$, we find from Eqs. (51), (52), and (55) that

$$\left[C_\perp-(\gamma_b mv_0)^2\right]_{\substack{C_z=\gamma_b mV_b\\ C_h=C_0}}=\left[1+\left(\frac{g}{r+f}\right)^2\right](p_r-p_r^0)^2 -\left[(\gamma_b mv_0')^2-\frac{F^2}{(r+f)^2+g^2}\right]\ , \tag{56}$$

where p_r^0 is defined by

$$p_r^0=\gamma_b mV_b\cos(\theta-k_0z)\frac{\omega_c}{\omega_0-\omega_c}\frac{\delta B}{B_0}\left[\frac{(r+f)^2+g^2-F/\gamma_b mV_b k_0}{(r+f)^2+g^2}\right]\ . \tag{57}$$

As a simple example, we consider the limit of zero perpendicular energy spread in Eq. (50). Making use of the identity

$$\delta(C_\perp-\gamma_b^2m^2v_0^2)=\lim_{\varepsilon\to0}\frac{1}{2\varepsilon}U[(C_\perp-\gamma_b^2m^2v_0^2)^2-\varepsilon^2]\ , \tag{58}$$

we find from Eqs. (50), (51), and (56) that the electron density profile $n_b^0(r,\theta,z)=\int_{-\infty}^{\infty}dp_r\int_{-\infty}^{\infty}dp_\theta\int_{-\infty}^{\infty}dp_z\ f_b^0(C_\perp,C_h,C_z)$ can be expressed as

$$n_b^0(r,\theta-k_0z)=\frac{n_0R_0\gamma_b mv_0}{[(r+f)^2+g^2]^{1/2}}\int_{-\infty}^{\infty}dp_r''\delta(p_r''^2-\psi)\ , \tag{59}$$

where $p_r''=\{1+[g/(r+f)]^2\}^{1/2}(p_r-p_r^0)$, and ψ is defined by

$$\psi(r,\theta-k_0z)=\left[(\gamma_b mv_0')^2-\frac{F^2}{(r+f)^2+g^2}\right]\ . \tag{60}$$

Carrying out the p_r'' integration in Eq. (59), the density profile can be expressed as

$$n_b^0(r,\theta-k_0z)=\begin{cases}\dfrac{n_0R_0v_0}{\{v_0'^2[(r+f)^2+g^2]-(F/\gamma_b m)^2\}^{1/2}}, & \psi \geq 0 ,\\ 0, \text{ otherwise} .\end{cases} \tag{61}$$

In the subsequent analysis it is useful to introduce the effective radial variable R defined by

$$R^2=\left(r+\frac{1}{k_0}\frac{\omega_c}{\omega_0-\omega_c}\frac{\delta B}{B_0}\sin(\theta-k_0z)\right)^2 + \frac{1}{k_0^2}\left(\frac{\omega_c}{\omega_0-\omega_c}\right)^2\left(\frac{\delta B}{B_0}\right)^2[1-\sin^2(\theta-k_0z)] , \tag{62}$$

and the constant quantities $r_L, \bar{R}, R_b^+$, and R_b^- defined by

$$r_L=\frac{v_0'}{\omega_c} , \tag{63}$$

$$\bar{R}^2=R_0^2\left[1-\left(\frac{2\omega_0}{\omega_c}-1\right)\left(\frac{\omega_c}{\omega_0-\omega_c}\right)^2\frac{1}{k_0^2R_0^2}\left(\frac{\delta B}{B_0}\right)^2\right] , \tag{64}$$

$$R_b^+=r_L+(\bar{R}^2+r_L^2)^{1/2} , \tag{65}$$

$$R_b^-=-r_L+(\bar{R}^2+r_L^2)^{1/2} . \tag{66}$$

Making use of Eqs. (61)-(66), and the definition of $\psi(r,\theta-k_0z)$ in Eq. (60), we find that the density profile in Eq. (61) can be expressed in the equivalent form

$$n_b^0(r,\theta-k_0z)=\begin{cases}\dfrac{n_0R_0\,2r_L(v_0/v_0')}{[(R_b^{+2}-R^2)(R^2-R_b^{-2})]^{1/2}}, & R_b^- \leq R \leq R_b^+ ,\\ 0 , \text{ otherwise} .\end{cases} \tag{67}$$

From Eqs. (61) and (67), note that the normalization of n_b^0 is such that $n_b^0=n_0=$const. for $r=R_0$ and $\delta B=0$. In addition, note from Eq. (67) that the beam density is singular at the inner ($R=R_b^-$) and outer ($R=R_b^+$)

boundaries of the electron beam. This is a consequence of the singular form for the perpendicular energy distribution function assumed in Eq. (58). For small but finite ε, the beam density remains finite and varies smoothly throughout the annulus.[9] We emphasize, however, that the beam density profile in Eq. (67) is integrable in the sense that the number of electrons per unit axial length, $N_b = \int_0^{2\pi} d\theta \int_0^{\infty} dr\, r\, n_b^0$ is finite. In any case, the equilibrium example in Eq. (67) is adequate for present purposes of describing the helical modulation of the inner and outer beam envelopes by the transverse wiggler field.

Making use of Eqs. (62), (65), (66), and (67), the outer boundary ($r=r_b^+$) and inner boundary ($r=r_b^-$) of the annular electron beam are determined from

$$r_b^+ = -\frac{1}{k_0}\frac{\omega_c}{\omega_0-\omega_c}\frac{\delta B}{B_0}\sin(\theta-k_0z) + \left\{\left[r_L+(\bar{R}^2+r_L^2)^{1/2}\right]^2 - \frac{1}{k_0^2}\left(\frac{\omega_c}{\omega_0-\omega_c}\right)^2\left(\frac{\delta B}{B_0}\right)^2[1-\sin^2(\theta-k_0z)]\right\}^{1/2} \tag{68}$$

and

$$r_b^- = -\frac{1}{k_0}\frac{\omega_c}{\omega_0-\omega_c}\frac{\delta B}{B_0}\sin(\theta-k_0z) + \left\{\left[-r_L+(\bar{R}^2+r_L^2)^{1/2}\right]^2 - \frac{1}{k_0^2}\left(\frac{\omega_c}{\omega_0-\omega_c}\right)^2\left(\frac{\delta B}{B_0}\right)^2[1-\sin^2(\theta-k_0z)]\right\}^{1/2}, \tag{69}$$

where $r_L=v_0'/\omega_c$ and $\bar{R}$ is defined in Eq. (64). In the special limiting case where $\delta B=0$, it follows from Eqs. (63) and (64) that $r_L=v_0/\omega_c$ and $\bar{R}=R_0$, and Eqs. (68) and (69) reduce to the familiar results[9]

$$(r_b^+)_{\delta B=0} = (R_0^2+r_L^2)^{1/2}+r_L\ , \tag{70}$$

and

$$(r_b^-)_{\delta B=0} = (R_0^2+r_L^2)^{1/2}-r_L\ . \tag{71}$$

That is, for $\delta B=0$, the average beam radius and beam thickness are constant, with $\bar{R}_b \equiv (r_b^+ + r_b^-)/2 = (R_0^2 + r_L^2)^{1/2} \simeq R_0$ (for $r_L^2 \ll R_0^2$), and $\Delta R_b \equiv r_b^+ - r_b^- = 2r_L$.

For the choice of equilibrium distribution function in Eq. (50) with $\varepsilon \to 0_+$, Eqs. (68) and (69) give very precise predictions for the inner and outer boundaries of the annular electron beam for $\delta B \neq 0$, within the context of the assumptions enumerated in Sec. II. In the remainder of this section, we make use of Eqs. (68) and (69) to examine the helical modulation of the beam envelope in the general case where δB is non-zero, assuming in addition that the dimensionless quantities

$$r_L^2/\bar{R}^2 < 1, \tag{72}$$

and

$$\frac{1}{k_0^2 R_0^2} \frac{\omega_0}{\omega_c} \left(\frac{\omega_c}{\omega_0 - \omega_c}\right)^2 \left(\frac{\delta B}{B_0}\right)^2 < 1, \tag{73}$$

can be treated as small parameters. In Eq. (72), $\bar{R}$ is defined in Eq. (64), and $r_L = 2v_0'/\omega_c$, where v_0' is defined in Eq. (53). In the regime of experimental interest $k_0^2 R_0^2 > 1$. In this regard, we note that the inequality in Eq. (73) is readily satisfied even for moderate wiggler amplitudes with $|\delta B/B_0| \lesssim 1$. This is true both for weak axial fields ($\omega_c \ll \omega_0$) and strong axial fields ($\omega_c \gg \omega_0$). Taylor expanding the expressions for $r_b^\pm$ in Eqs. (68) and (69), and retaining terms to order $(r_L^2/\bar{R}^2)$ and $(\delta B/B_0)^2$, we obtain the approximate expressions

$$\begin{aligned} r_b^\pm = \bar{R} + \bar{R} \left\{ \pm \frac{r_L}{\bar{R}} - \frac{1}{k_0 \bar{R}} \frac{\omega_c}{\omega_0 - \omega_c} \frac{\delta B}{B_0} \sin(\theta - k_0 z) \right\} \\ + \frac{1}{2} \bar{R} \left\{ \frac{r_L^2}{\bar{R}^2} - \frac{1}{k_0^2 \bar{R}^2} \left(\frac{\omega_c}{\omega_0 - \omega_c}\right)^2 \left(\frac{\delta B}{B_0}\right)^2 [1 - \sin^2(\theta - k_0 z)] \right\} . \end{aligned} \tag{74}$$

Evidently, from Eq. (74), the beam thickness $\Delta R_b = r_b^+ - r_b^-$ is given by

$$\Delta R_b = 2r_L = \frac{2v_0'}{\omega_c} , \tag{75}$$

correct to order $(r_L/\bar{R})^2$ and $(\delta B/B_0)^2$. In Eq. (75), v_0' is defined in Eq. (53). Moreover, the average beam radius $\bar{R}_b = (r_b^+ + r_b^-)/2$ is given by

$$\begin{aligned} \bar{R}_b = \bar{R} \left\{ 1 - \frac{1}{k_0 \bar{R}} \frac{\omega_c}{\omega_0 - \omega_c} \frac{\delta B}{B_0} \sin(\theta - k_0 z) \right\} \\ + \frac{1}{2} \bar{R} \left\{ \frac{r_L^2}{\bar{R}^2} - \frac{1}{k_0^2 \bar{R}^2} \left(\frac{\omega_c}{\omega_0 - \omega_c} \right)^2 \left(\frac{\delta B}{B_0} \right)^2 [1 - \sin^2(\theta - k_0 z)] \right\} , \end{aligned} \tag{76}$$

correct to order $(r_L/\bar{R})^2$ and $(\delta B/B_0)^2$. We note from Eq. (76) that the leading-order modulation of the average beam radius $\bar{R}_b$ is linear in δB. Therefore, making use of Eq. (64), the expression for $\bar{R}_b$ in Eq. (76) can be approximated by

$$\bar{R}_b = \bar{R} \left\{ 1 - \frac{1}{k_0 \bar{R}} \frac{\omega_c}{\omega_0 - \omega_c} \frac{\delta B}{B_0} \sin(\theta - k_0 z) \right\} , \tag{77}$$

correct to lowest order in $\delta B/B_0$.

As a numerical example, in Fig. 2 we show a plot of the normalized average beam radius $k_0 \bar{R}_b$ (dashed curve) versus $\theta - k_0 z$ obtained from Eq. (77) for several values of $\delta B/B_0$ and the choice of equilibrium parameters $\omega_0 = 4\omega_c$, $v_0^2/c^2 = 0.04$, $k_0 R_0 = 3/2$, $k_0 r_L^0 = k_0 v_0/\omega_c = 1/20$, $\gamma_b = 3$ and $V_b^2/c^2 = 8/9$. In this case

$$k_0 \Delta R_b = 0.1 \left[1 + \frac{200}{81} \left(\frac{\delta B}{B_0} \right)^2 \right]^{1/2} , \tag{78}$$

and

$$k_0 \bar{R}_b = k_0 \bar{R} - \frac{1}{3} \frac{\delta B}{B_0} \sin(\theta - k_0 z) , \tag{79}$$

follow from Eqs. (53), (75), and (77). Here, $k_0 \bar{R} = k_0 R_0 [1 + (28/81)(\delta B/B_0)^2]^{1/2}$ follows from Eq. (64). Equations (78) and (79) yield the results shown

in Fig. 2 for $\delta B/B_0=1/4$ [Fig. 2(a)], $\delta B/B_0=0.5$ [Fig. 2(b)] and $\delta B/B_0=1$ [Fig. 2(c)]. From Eq. (79), we define the peak amplitude of the radial modulation by $k_0\bar{\Delta}R_b = |(1/3)(\delta B/B_0)|$. We note from Fig. 2 and Eqs. (78) and (79) that the normalized beam thickness $k_0\Delta R_b$ and maximum modulation amplitude $k_0\bar{\Delta}R_b$ increase from $(k_0\Delta R_b, k_0\bar{\Delta}R_b)=(0.10, 0)$ for $\delta B=0$, to $(k_0\Delta R_b, k_0\bar{\Delta}R_b)=(0.19, 0.33)$ for $\delta B/B_0=1$.

In concluding this section, we emphasize that the theoretical model developed here can be used to calculate the equilibrium properties of a helically modulated annular electron beam propagating in the equilibrium magnetic field $B_0\hat{e}_z-\delta B\cos k_0 z\hat{e}_x-\delta B\sin k_0 z\hat{e}_y$ for a broad range of system parameters ω_c, ω_0, v_0^2/c^2, $\delta B/B_0$, k_0R_0, etc. As in Sec. II.A, the major approximations relate to the assumptions that the transverse electron motion is nonrelativistic [Eq. (12)] and that the axial motion is far removed from cyclotron resonance [Eq. (14)].

IV. CONCLUSIONS

In this paper we have developed a self-consistent Vlasov description of helically distorted relativistic electron beam equilibria for free electron laser applications. In particular, we have considered radially confined equilibria for a helically distorted relativistic electron beam propagating in the combined transverse wiggler and uniform axial guide fields described by Eqs. (1) and (2). Assuming that the beam density and current are sufficiently small that equilibrium self fields can be neglected in comparison with $B_0\hat{e}_z+\delta\underset{\sim}{B}$, it is found that there are three useful and exact invariants $(C_\perp, C_h, C_z)$ associated with single-particle motion in the equilibrium field configuration. These invariants are used to construct radially confined Vlasov equilibria $f_b^0(C_\perp, C_h, C_z)$ for an intense relativistic electron beam propagating primarily in the z-direction. Specific examples of solid [Eq. (20)] and hollow [Eq. (50)] beam equilibria are analyzed in Sec. III, and it is shown that the transverse wiggler field can have a large modulational influence on the beam envelope, depending on the size of $\delta B/B_0$. We believe that the present equilibrium investigations form an important first step in formulating a self-consistent Vlasov description of the free electron laser instability that both includes the effects of finite radial geometry and correctly incorporates the nonlinear influence of the transverse wiggler field on the beam equilibrium.

ACKNOWLEDGMENT

This research was supported in part by the Office of Naval Research, Contract No. N00014-79-C-0555, and in part by the Office of Naval Research under the auspices of a Joint Program with the Naval Research Laboratory. The research of one of the authors (H.S.U.) was supported by the Independent Research Fund at the Naval Surface Weapons Center.

V. REFERENCES

1. P. Sprangle, J. Plasma Phys. 11, 299 (1974).
2. T. Kwan and J. M. Dawson, Phys. Fluids 22, 1089 (1979).
3. R. C. Davidson and H. S. Uhm, "Self-Consistent Vlasov Description of the Free Electron Laser Instability in a Relativistic Electron Beam with Uniform Density", Phys. Fluids 23, in press (1980).
4. I. B. Bernstein and J. L. Hirshfield, Phys. Rev. 20A, 1661 (1979).
5. P. Sprangle and R. A. Smith, NRL Memorandum Report 4033 (1979).
6. T. C. Marshall, S. Talmadge, and P. Efthimion, Appl. Phys. Lett. 31, 320 (1977).
7. D. A. G. Deacon, L. R. Elias, J. M. M. Madey, G. J. Ramian, H. A. Schwettman, and T. I. Smith, Phys. Rev. Lett. 38, 897 (1977).
8. R. C. Davidson, Theory of Nonneutral Plasmas (Benjamin, Reading, Mass., 1974).
9. H. S. Uhm and R. C. Davidson, Phys. Fluids 22, 1804 (1979).

FIGURE CAPTIONS

Fig. 1 Plot of $k_0 R_b$ [Eq. (30)] versus $\theta - k_0 z$ for $\omega_0 = 4\omega_c$, $\omega_b = 0.1\ \omega_c$, $v_0^2/c^2 = 0.04$, $\gamma_b = 3$, $V_b^2/c^2 = 8/9$ and (a) $\delta B/B_0 = 1/4$, (b) $\delta B/B_0 = 1/2$, and (c) $\delta B/B_0 = 1$.

Fig. 2 Plot of $k_0 \bar{R}_b$ [Eq. (77)] versus $\theta - k_0 z$ for $\omega_0 = 4\omega_c$, $v_0^2/c^2 = 0.04$, $\gamma_b = 3$, $V_b^2/c^2 = 8/9$, $k_0 R_0 = 3/2$, $k_0 r_L^0 = 1/20$, and (a) $\delta B/B_0 = 1/4$, (b) $\delta B/B_0 = 1/2$, and (c) $\delta B/B_0 = 1$.

APPENDIX A

SINGLE-PARTICLE CONSTANTS OF THE MOTION

In this appendix, we consider the motion of an individual electron in the applied magnetic field

$$\underset{\sim}{B}^0 = B_0\hat{\underset{\sim}{e}}_z - \delta B\cos k_0 z\,\hat{\underset{\sim}{e}}_x - \delta B\sin k_0 z\,\hat{\underset{\sim}{e}}_y$$

$$= B_0\hat{\underset{\sim}{e}}_z - \delta B\cos(\theta - k_0 z)\hat{\underset{\sim}{e}}_r + \delta B\sin(\theta - k_0 z)\hat{\underset{\sim}{e}}_\theta \ ,$$

where B_0=const. is the uniform axial field, $\delta\underset{\sim}{B} = -\delta B\cos(\theta - k_0 z)\hat{\underset{\sim}{e}}_r + \delta B\sin(\theta - k_0 z)\hat{\underset{\sim}{e}}_\theta$ is the transverse helical wiggler field expressed in cylindrical polar coordinates, δB=const. is the wiggler amplitude, and $\lambda_0 = 2\pi/k_0$ is the wavelength. Making use of $\gamma' = (1+\underset{\sim}{p}'^2/m^2c^2)^{1/2}$=const., the equations of motion for the particle orbits r'(t'), θ'(t') and z'(t') can be expressed as

$$\gamma' m\left(\frac{d^2}{dt'^2}\, r' - r'\left(\frac{d\theta'}{dt'}\right)^2\right) = -\frac{eB_0}{c}\, r'\, \frac{d\theta'}{dt'} + \frac{e\delta B}{c}\sin(\theta' - k_0 z')\, \frac{dz'}{dt'} \tag{A.1}$$

$$\gamma' m\left(r'\, \frac{d^2}{dt'^2}\, \theta' + 2\left(\frac{dr'}{dt'}\right)\left(\frac{d\theta'}{dt'}\right)\right) = \frac{eB_0}{c}\, \frac{dr'}{dt'} + \frac{e\delta B}{c}\cos(\theta' - k_0 z')\, \frac{dz'}{dt'} \tag{A.2}$$

$$\gamma' m\, \frac{d^2 z'}{dt'^2} = -\frac{e\delta B}{c}\sin(\theta' - k_0 z')\, \frac{dr'}{dt'} - \frac{e\delta B}{c}\cos(\theta' - k_0 z')\, r'\, \frac{d\theta'}{dt'} \ . \tag{A.3}$$

Conservation of energy (γ'=const.) of course implies that

$$p_r'^2 + p_\theta'^2 + p_z'^2 = \text{const.}, \tag{A.4}$$

where $p_r' = \gamma' m dr'/dt'$, $p_\theta' = \gamma' m r' d\theta'/dt'$ and $p_z' = \gamma' m dz'/dt'$. Moreover,

multiplying Eq. (A.2) by r' and making use of Eq. (A.3) gives

$$\frac{d}{dt'}\left[r'\left(p'_\theta - \frac{1}{2}\frac{eB_0}{c}r'\right)\right] = \frac{e\delta B}{c}r'\cos(\theta'-k_0z')\frac{dz'}{dt'}$$

$$= -\frac{d}{dt'}\left[\frac{e\delta B}{ck_0}r'\sin(\theta'-k_0z')\right] - \frac{\gamma'm}{k_0}\frac{d^2z'}{dt'^2} \quad . \tag{A.5}$$

Integrating Eq. (A.5) with respect to t' gives the helical invariant

$$P'_\theta + \frac{p'_z}{k_0} + \frac{e\delta B}{ck_0}r'\sin(\theta'-k_0z') = \text{const.}, \tag{A.6}$$

where $p'_z=\gamma'mdz'/dt'$, and $P'_\theta=r'(p'_\theta-eB_0r'/2c)$ is the canonical angular momentum associated with the applied axial field B_0. Subtracting $\gamma_b mV_b/k_0=$const. from Eq. (A.6), where $\gamma_b mc^2$ is the characteristic directed beam energy and V_b is the characteristic mean axial velocity of the beam electrons, gives

$$C_h = P'_\theta + \frac{1}{k_0}(p'_z-\gamma_b mV_b) + \frac{e\delta B}{ck_0}r'\sin(\theta'-k_0z') = \text{const.}, \tag{A.7}$$

which is the form of the helical invariant used in Secs. II and III [Eq. (5)].

To determine the axial invariant associated with Eqs. (A.1)-(A.3), we consider the quantity I_z defined by

$$I_z = (p'_z)^2 - \frac{2eB_0}{ck_0}p'_z + \frac{2e}{ck_0}p'_r\delta B\cos(\theta'-k_0z')$$

$$- \frac{2e}{ck_0}p'_\theta\delta B\sin(\theta'-k_0z') \ , \tag{A.8}$$

where $p'_z=\gamma'mdz'/dt'$, $p'_r=\gamma'mdr'/dt'$ and $p'_\theta=\gamma'mr'\ d\theta'/dt'$. Differentiating Eq. (A.8) with respect to t' and making use of Eq. (A.3) gives

$$\frac{dI_z}{dt'} = -2\left(p_z' - \frac{eB_0}{ck_0}\right)\frac{e\delta B}{c}\left[\sin(\theta'-k_0z')\,\frac{dr'}{dt'}\right.$$

$$\left.+\cos(\theta'-k_0z')r'\,\frac{d\theta'}{dt'}\right] + \frac{2e}{ck_0}\,\delta B\left[\frac{dp_r'}{dt'}\cos(\theta'-k_0z')\right. \tag{A.9}$$

$$-\frac{dp_\theta'}{dt'}\sin(\theta'-k_0z') - p_r'\sin(\theta'-k_0z')\left(\frac{d\theta'}{dt'}-k_0\frac{dz'}{dt'}\right)$$

$$\left.-p_\theta'\cos(\theta'-k_0z')\left(\frac{d\theta'}{dt'}-k_0\frac{dz'}{dt'}\right)\right] .$$

Substituting Eqs. (A.1) and (A.2) into Eq. (A.9) and combining terms gives

$$\frac{dI_z}{dt'} = 0 , \tag{A.10}$$

which implies that I_z=const. is an exact single-particle invariant. Adding $(eB_0/ck_0)^2$ to Eq. (A.8) implies that

$$\left(p_z' - \frac{eB_0}{ck_0}\right)^2 - \frac{2e}{ck_0}\,\delta B[p_\theta'\sin(\theta'-k_0z') - p_r'\cos(\theta'-k_0z')]$$

$$= \left(C_z - \frac{eB_0}{ck_0}\right)^2 = \text{const.}, \tag{A.11}$$

which is the form of the exact axial invariant used in Secs. II and III [Eq. (6)]. For $\delta B \to 0$, we note from Eq. (A.11) that C_z reduces to the axial momentum p_z'.

Finally, subtracting $I_z + 2(eB_0/ck_0)\gamma_b mV_b$=const., from Eq. (A.4) gives

$$C_\perp = p_r'^2 + p_\theta'^2 + \frac{2eB_0}{ck_0}\,(p_z' - \gamma_b mV_b)$$

$$-\frac{2e}{ck_0}\,p_r'\delta B\cos(\theta'-k_0z') + \frac{2e}{ck_0}\,p_\theta'\delta B\sin(\theta'-k_0z) = \text{const.}, \tag{A.12}$$

which is the form of the exact perpendicular invariant used in Secs. II and III [Eq. (4)].

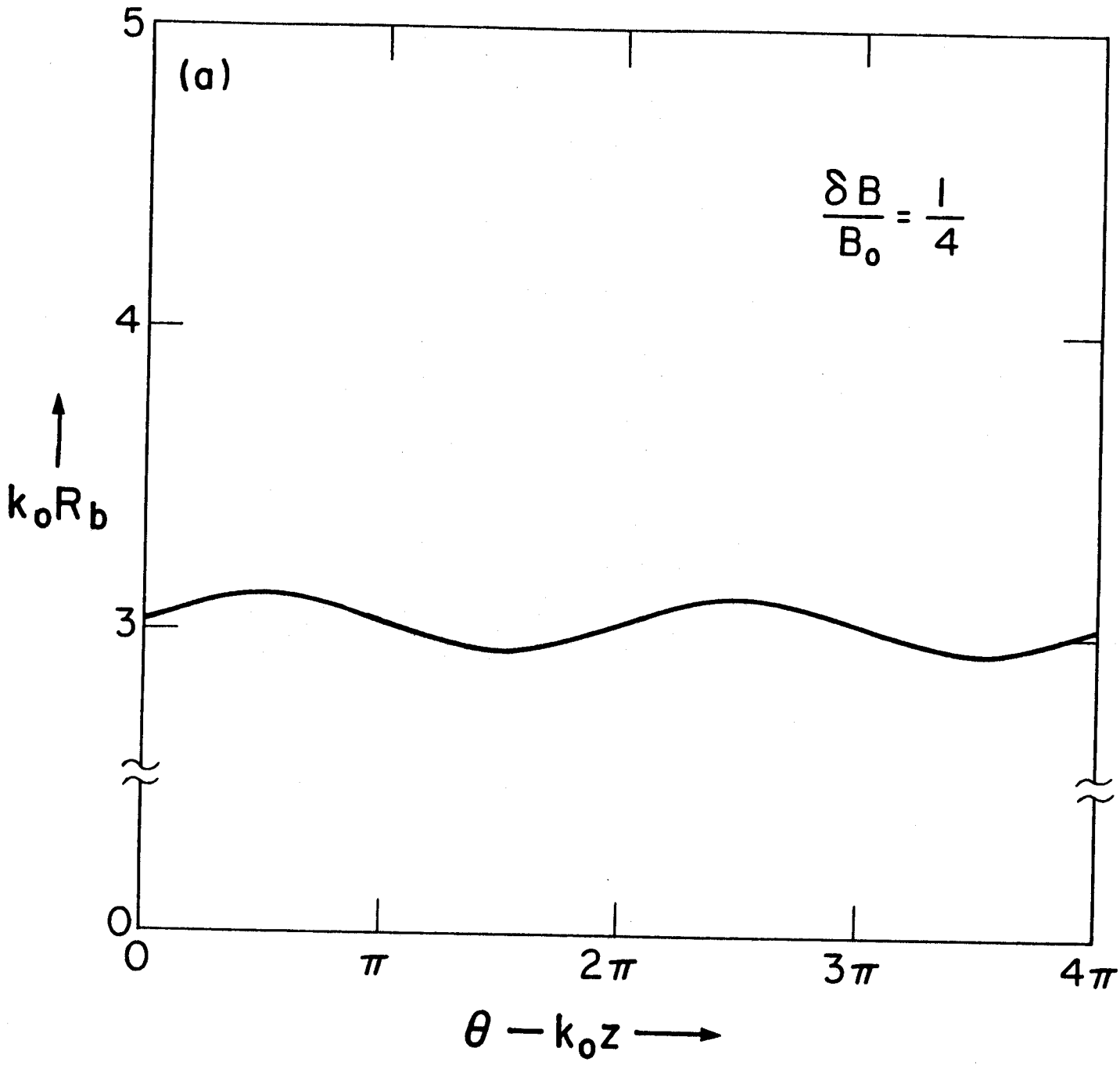

Fig. 1(a)

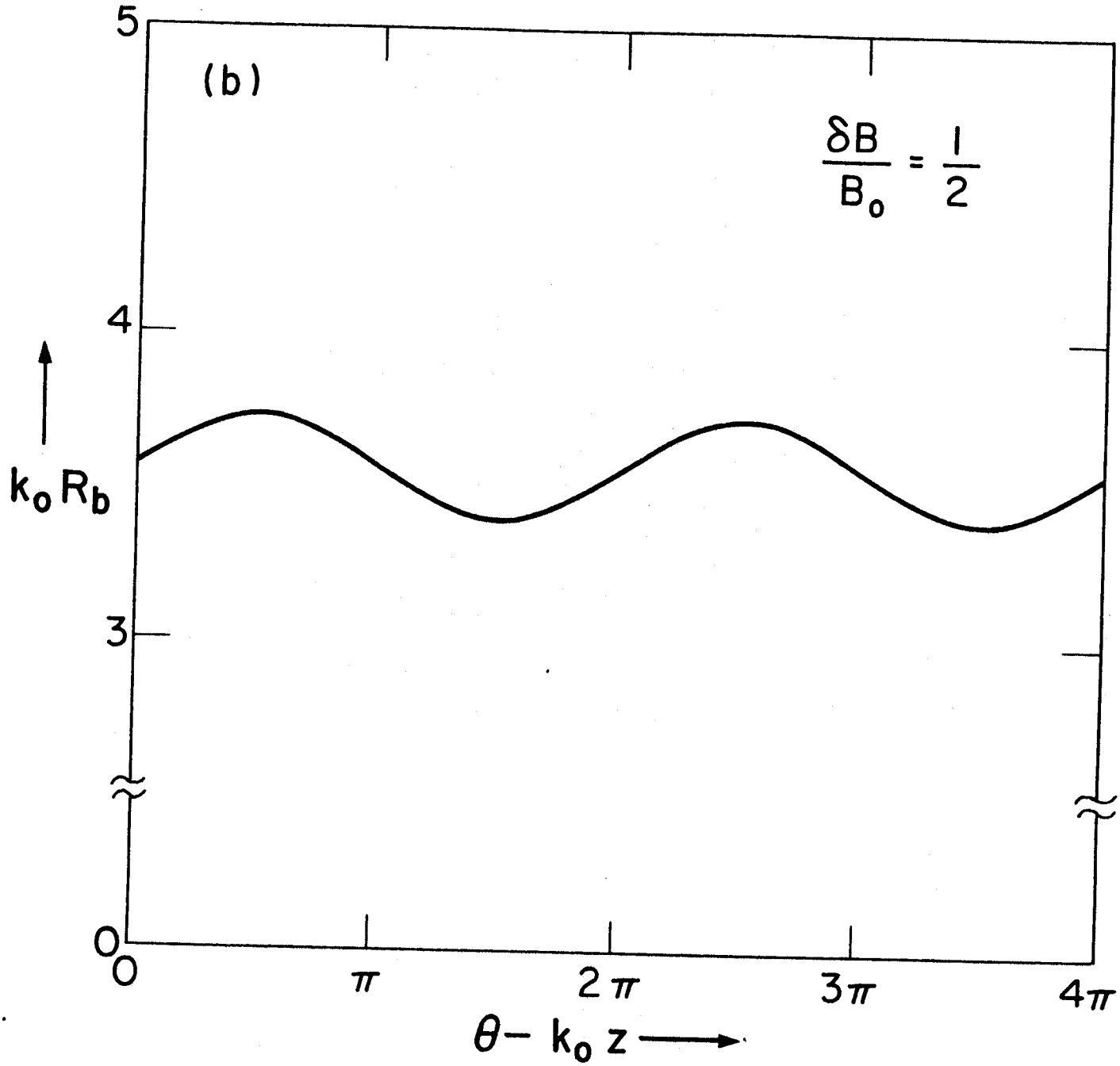

Fig. 1(b)

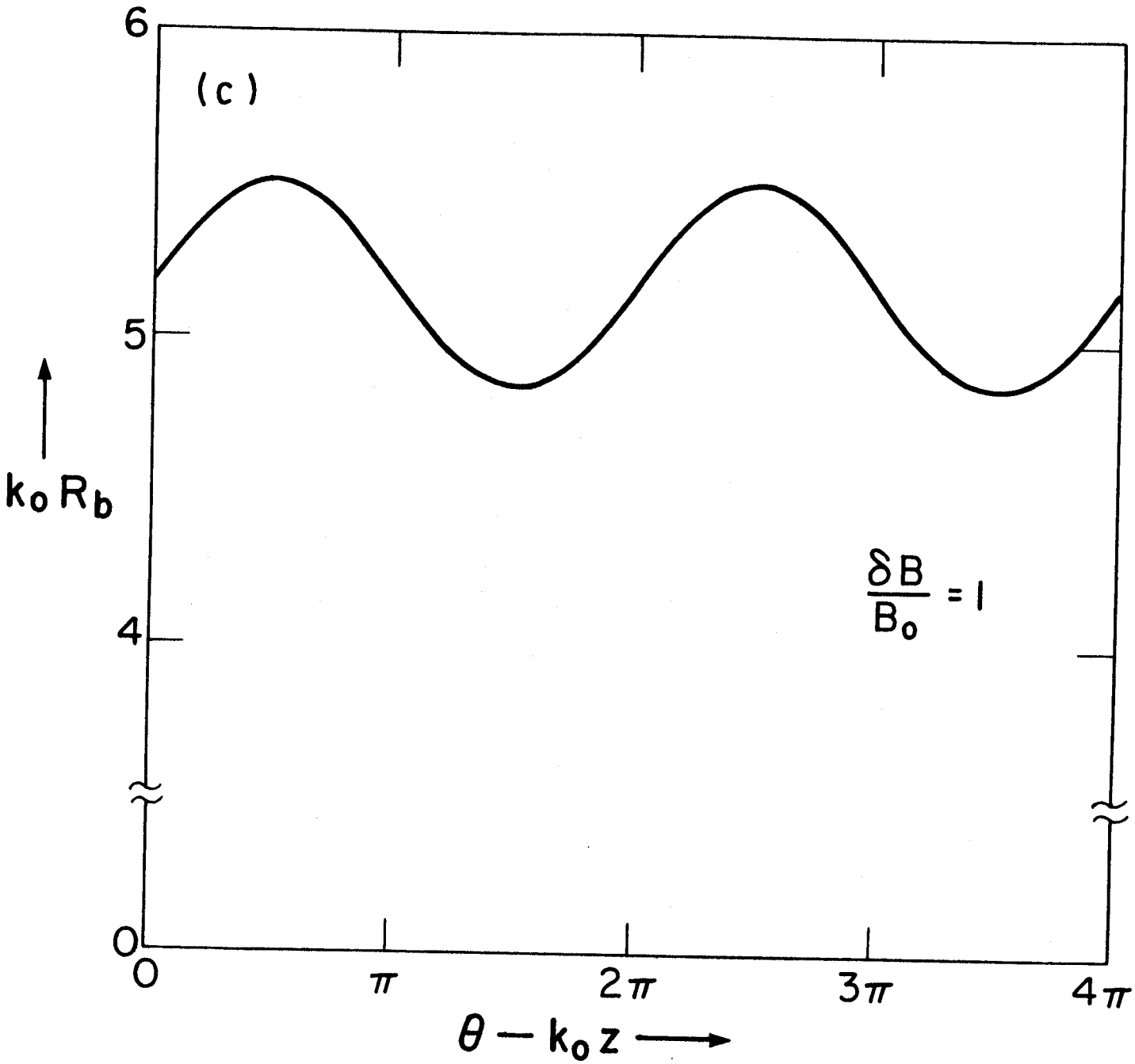

Fig. 1(c)

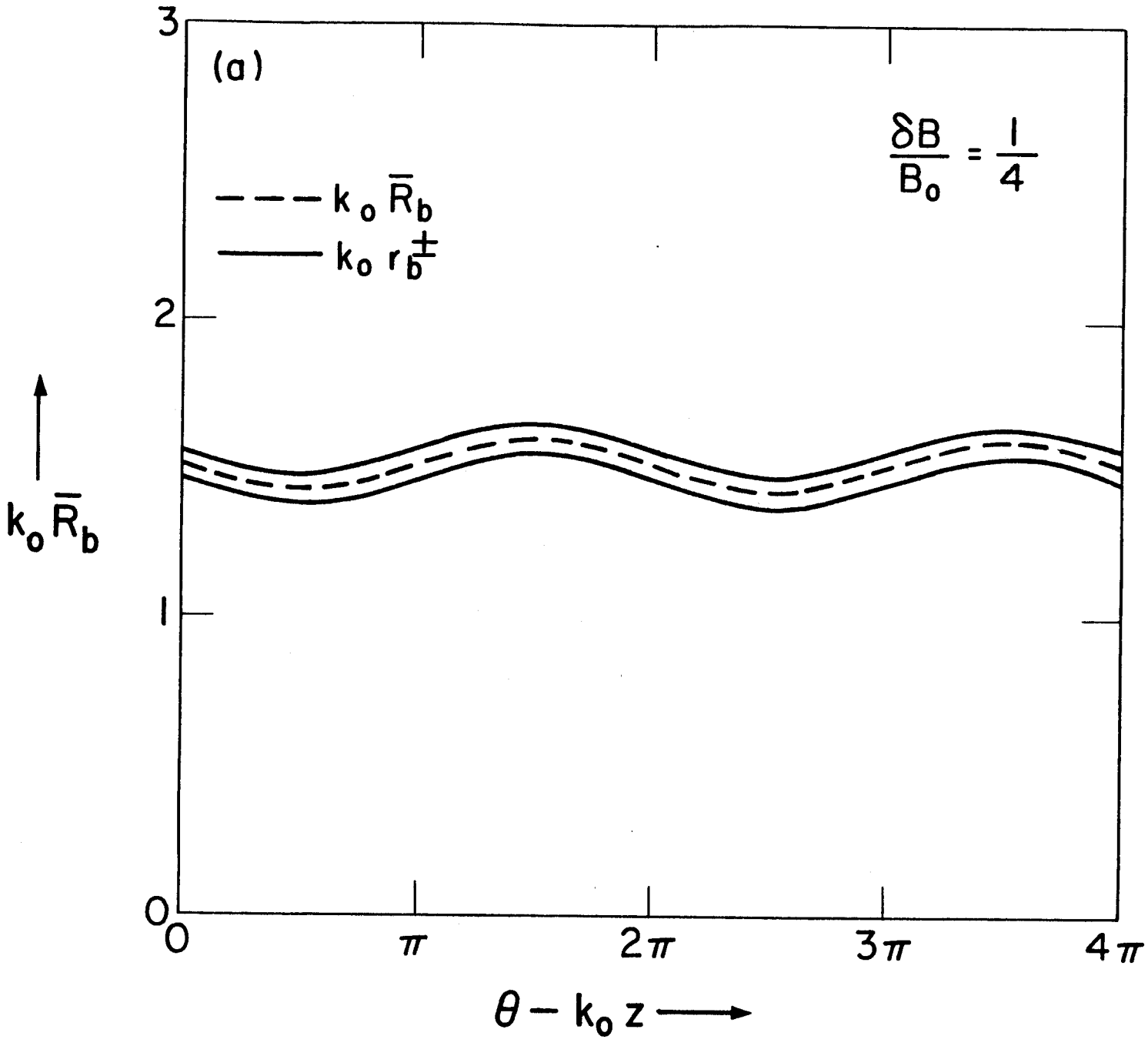
3
(a)
$\frac{\delta B}{B_o} = \frac{1}{4}$
$k_o \bar{R}_b$
$k_o r_b^{\pm}$
2
$k_o \bar{R}_b$
1
0
0
π
2π
3π
4π
$\theta - k_o z \longrightarrow$

Fig. 2(a)

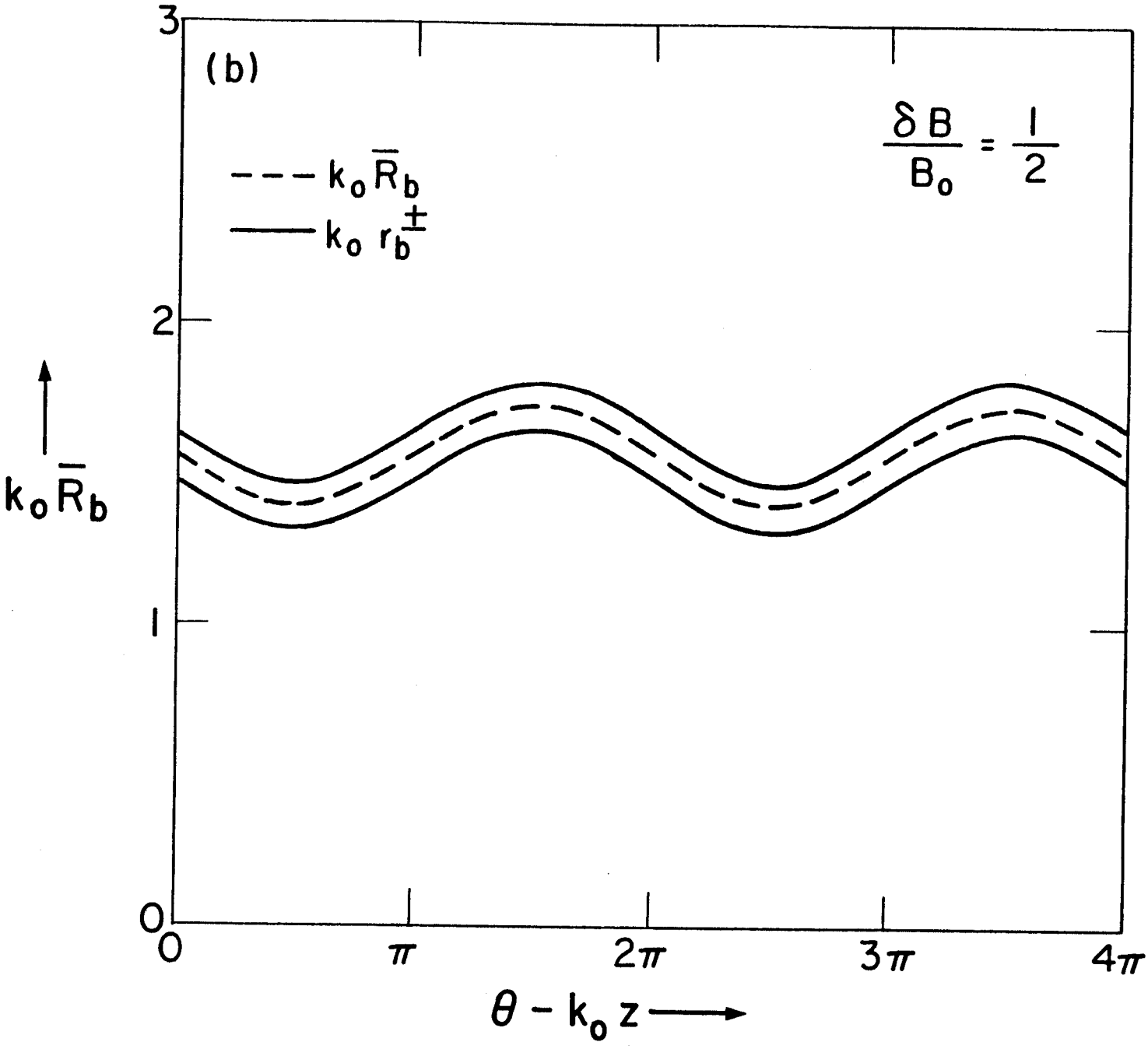
(b)
$\frac{\delta B}{B_o} = \frac{1}{2}$
$k_o \bar{R}_b$
$k_o r_b^{\pm}$
$k_o \bar{R}_b$
3
2
1
0
0
π
2π
3π
4π
$\theta - k_o z$

Fig. 2(b)

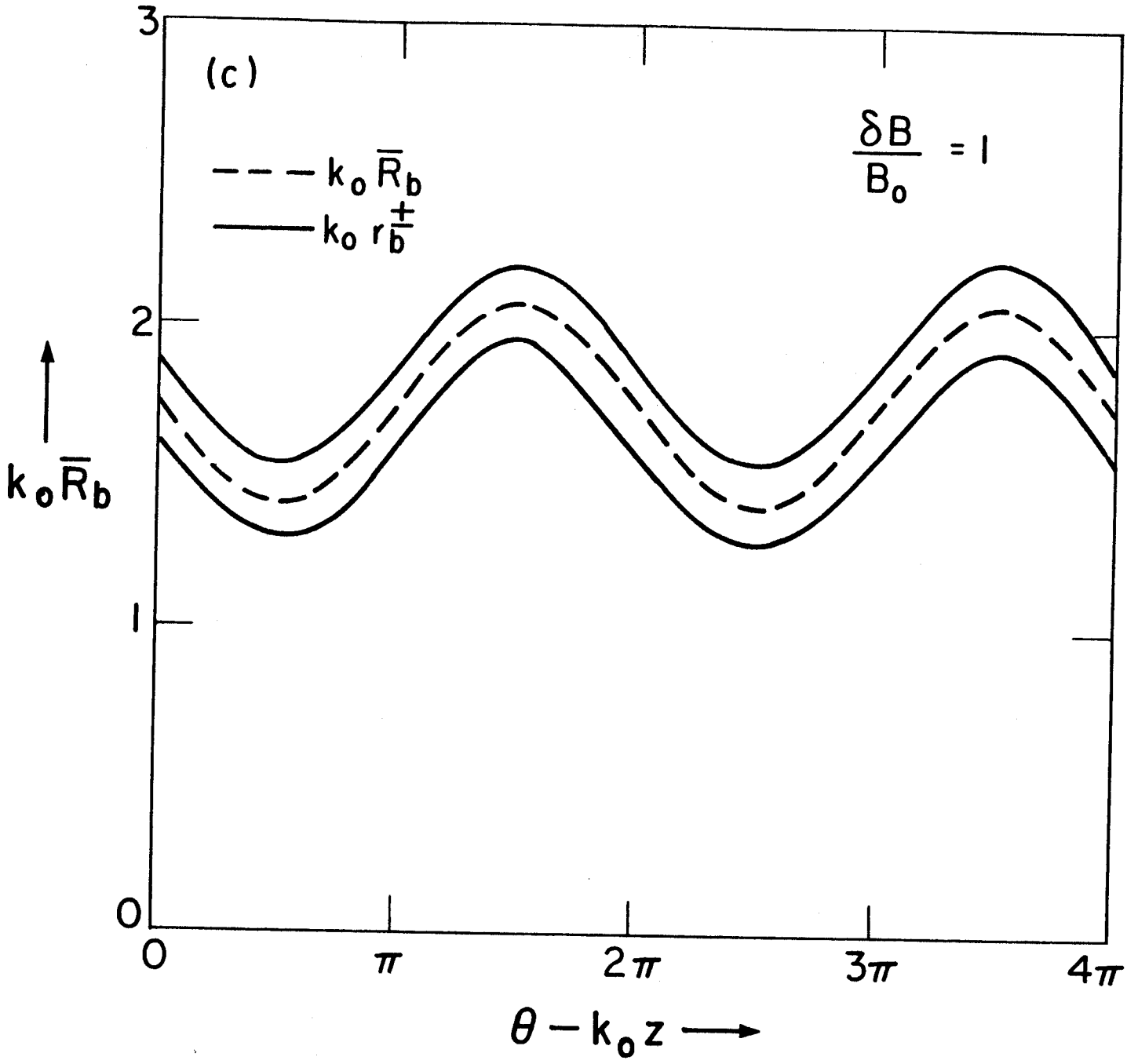
(c)
$\frac{\delta B}{B_o} = 1$
$k_o \bar{R}_b$
$k_o r_b^{\pm}$
$k_o \bar{R}_b$
3
2
1
0
0
π
2π
3π
4π
$\theta - k_o z$

Fig. 2(c)